Journal of Biochemical and Molecular Toxicology

WILEY

RESEARCH ARTICLE

Heme Oxygenase-1 Mediated Protective Effects of Linalool on Rifampicin-Induced Spleen Toxicity Through the PI3K/Akt Pathway

Ayşegül Acet[1] | Sebile Azırak[2] | Ebru Annaç[3] | İbrahim Bozgeyik[1] | Halime Tozak Yıldız[4] | Deniz Taştemir Korkmaz[1]

[1]Department of Medical Biology, Faculty of Medicine, Adıyaman University, Adıyaman, Turkey | [2]Vocational School of Health Services, Adıyaman University, Adıyaman, Turkey | [3]Department of Histology and Embryology, Faculty of Medicine, Adıyaman University, Adıyaman, Turkey | [4]Department of Histology and Embryology, Faculty of Medicine, Kırşehir Ahi Evran University, Kırşehir, Turkey

Correspondence: Deniz Taştemir Korkmaz (dtastemir@adiyaman.edu.tr)

Received: 10 April 2025 | **Revised:** 24 November 2025 | **Accepted:** 23 December 2025

Keywords: HO-1 | Linalool | oxidative stress | rifampicin | spleen

ABSTRACT

Rifampicin (RF) is a primary anti-tuberculosis medication utilized in tuberculosis treatment, and its concurrent administration with other medications, as well as the duration of therapy, may result in adverse effects. While the hepatotoxicity of RF is established, its impact on the spleen remains unexamined. Thus, our study aimed to investigate the impact of RF on the spleen and the protective role of Linalool (LN), a monoterpene, through the Heme oxygenase-1 (HO-1) enzyme pathway, with biochemical analyses, oxidative stress parameters, protein levels, and histopathological assessments. In the study, thirty healthy adult male Sprague-Dawley rats were randomly allocated into five groups: control, solvent control (dimethyl sulfoxide - DMSO), RF, LN, and RF + LN. Spleen tissues and blood specimens were collected from the rats for examination. RF markedly elevated total and indirect bilirubin, Fe^{2+}, HO-1, and MDA levels, while diminishing GSH levels. Conversely, in the RF + LN group, total and indirect bilirubin, Fe^{2+}, HO-1, and MDA levels were dramatically reduced, whereas GSH levels were elevated. Histopathologically, RF-induced defects were ameliorated in the LN-treated cohorts. In conclusion, rifampicin exhibited toxic effects on the spleen, which were mitigated by LN.

1 | Introduction

Tuberculosis (TB) is a preventable and treatable illness caused by *Mycobacterium tuberculosis*, mostly affecting the pulmonary system. In 2023, tuberculosis resulted in 1.3 million fatalities, positioning it as the second foremost infectious cause of mortality globally, following COVID-19 [1]. The first-line anti-tuberculosis (ATD) drugs—rifampicin (RF), isoniazid, pyrazinamide and ethambutol—are crucial for the treatment of TB. The combination and duration of treatment depends on whether the patient has active or latent disease [2]. Among these, RF is particularly important due to its potent bactericidal efficacy against *Mycobacterium tuberculosis*.

RF, a semi-synthetic derivative of rifamycin, is a crucial drug for TB therapy; yet, it may induce various adverse consequences when administered at prolonged or elevated doses. One of the most notable is hepatotoxicity, which can lead to liver damage and, in severe cases, liver failure [3]. The mechanisms behind this include oxidative stress (OS), mitochondrial dysfunction, and cholestasis. Additionally, RF can induce allergic reactions, gastrointestinal difficulties, flu-like symptoms, blood abnormalities, and renal toxicity. It may also alter the color of physiological fluids and interact with other drugs, potentially intensifying its harmful effects and requiring vigilant patient monitoring [4, 5]. Sharma and Sharma (2017) noted that ATDs have harmful effects on other organs beyond the liver, including the kidneys,

testes, ovaries, blood, bones and spleen. Nonetheless, investigations regarding the toxicity of ATDs on the spleen are few [6].

The spleen, the largest lymphoid organ in the body, plays a critical role in regulating both local and systemic immune responses. It is anatomically connected to the liver via the portal vein system and contains specialized lymphocytes and myeloid cells organized into distinct functional regions [7]. Notably, the spleen expresses high levels of heme oxygenase-1 (HO-1), a cytoprotective enzyme involved in heme degradation and OS regulation [8]. This makes the spleen a key organ for studying the systemic effects of rifampicin toxicity.

HO-1 is a crucial antioxidant regulated by nuclear factor erythroid 2-related factor 2 (Nrf2) and is vital in safeguarding cellular redox equilibrium against oxidative stress. Nrf2 is activated by various signaling pathways, including phosphatidylinositol 3-kinase (PI3K), protein kinase C (PKC), c-Jun N-terminal kinase (JNK), and mitogen-activated protein kinase (MAPK), to evade KEAP1 repression, translocate to the nucleus, and stimulate the expression of multiple antioxidant enzymes, such as HO-1 [9, 10]. HO-1 is a rate-limiting enzyme in the heme degradation pathway, converting hemoglobin into biliverdin, free iron and carbon monoxide (CO). Biliverdin is then reduced to bilirubin via biliverdin reductase. Both biliverdin and bilirubin possess antioxidant properties, while CO acts as a signaling molecule influencing inflammation, apoptosis and injury [11]. High levels of HO-1 are found in the spleen, liver, and bone marrow, particularly in tissues involved in erythrocyte turnover [8].

Nowadays, there is a growing interest in natural products as potential therapeutic agents from medicinal plants [12–15]. Linalool (LN), a monoterpene alcohol present in various plants including coriander, rosewood, basil, mint, ginger, laurel, thyme, sage, nutmeg, and cinnamon [16–18], demonstrates a diverse array of biological activities, encompassing antioxidant, anti-inflammatory, and neuroprotective properties [19]. Due to these properties, we used LN to alleviate OS caused by RF in this study.

This study aims to examine the potential protective effects of LN against RF-induced toxicity, specifically targeting the spleen. By exploring the role of HO-1 in mitigating OS and cellular damage, this study hopes to gain insights into the mechanisms behind RF toxicity and examines the therapeutic potential of natural products like LN.

2 | Materials and Methods

2.1 | Chemicals

RF (purity > 98%) was acquired from TCI chemicals (India) (CAS 13292-46-1), and the ELISA kit for HO-1 was obtained from USCN (Wuhan USCN Business Co. Ltd) (Lot: L220525431). LN and the additional compounds utilized in the study were sourced from Sigma-Aldrich (USA).

2.2 | Ethical Approval

This study was approved by the Animal Experiments Local Ethics Committee of Adıyaman University (Protocol no #2022/028). All experimental protocols adhered to the National Institutes of Health Guidelines for the Care and Use of Laboratory Animals (NIH Publications No. 8023, revised 1978) and the ARRIVE Guidelines.

2.3 | Animal Assemblages and Treatments

A total of 30 adult male Sprague Dawley rats weighing 250–300 g were used in this study. The subjects were accommodated in polycarbonate enclosures maintained under a typical 12-h light/dark cycle at 24°C with a relative humidity of 42 ± 5%. They were divided into five groups with six rats in each group. The groups and treatments [20, 21] are presented in Table 1.

On the 16th day, the rats were anesthetized with ketamine–xylazine (50 mg/kg–5 mg/kg). Blood samples were obtained by heart puncture under anesthetic conditions and centrifuge at 4500 g for 10 min to separate the serum for biochemical analysis and Enzyme-linked Immunosorbent Assay (ELISA). After that, the rats were sacrificed by exsanguination and their spleens were removed for subsequent analysis. One half of the spleen was immersed in 10% neutral formalin for histopathological examination, while the remaining half was preserved at −80°C for subsequent assessment of OS.

2.4 | Tissue Homogenization

Tissue homogenates from 0.3 to 0.5 g of spleen tissues were prepared by an Ultra-Turrax homogenizer (~10 s) in ice-cooled plastic tubes containing PBS at a weight:volume ratio of 1:9 and centrifuged at 4000 rpm for 8 min at 4°C. The supernatants were removed and used for ELISA and OS biomarkers. Homogenization was done just before starting the tests.

2.5 | Assessment of Oxidative Stress Biomarkers

MDA concentrations were quantified to evaluate OS and lipid peroxidation levels. Spleen MDA levels were measured based on the relative production of thiobarbituric acid (TBA) reactive substances [22]. After homogenization of the spleen tissue,

TABLE 1 | Study groups and treatments.

Study Groups ($n = 6$ in each group)	Treatment(s)
Control	No treatment
DMSO (solvent control)	50 mg/kg/day DMSO by gavage for 15 days
RF	50 mg/kg/day RF by gavage for 15 days [20]
LN	50 mg/kg/day LN intraperitoneally for 15 days [21]
RF + LN	50 mg/kg/day LN intraperitoneally and 50 mg/kg/day RF by gavage for 15 days.

Abbreviations: DMSO, dimethyl sulfoxide; LN, linalool; RF, rifampicin.

0.25 mL of the supernatant was taken, placed in a glass tube and the trichloroacetic acid (TCA)/TBA (3:1 v/v) mix reagent was added. After thorough vortexing, the tubes were placed on a metal spore and kept in a 100°C water bath for 20 min. At the end of the time, the tubes were allowed to cool in cold water. The cooled tubes were centrifuged at 3000–5000 rpm for 5 min. The supernatant was read against the blind at 532 nm in a spectrophotometer (UV mini-1240; Shimadzu, Tokyo, Japan).

Glutathione (GSH) levels were determined using the method outlined by Ellman (1959) [23]. In this experiment, 5,5'-dithiobis-2-nitrobenzoic acid (DTNB) was introduced to the homogenized material, leading to the development of a yellow-green color due to its interaction with GSH. The concentration of reduced GSH was quantified by measuring the absorbance at 410 nm with a spectrophotometer (UV mini-1240; Shimadzu, Tokyo, Japan).

2.6 | ELISA for HO-1

An ELISA kit for HO-1 levels was utilized to quantify HO-1 protein in serum and spleen tissue. The experiment was conducted in accordance with the manufacturer's guidelines. Prior to the study, blank and standard solutions (10, 5, 2.5, 1.25, 0.625, 0.312, and 0.156 ng/mL) together with reagents were prepared (7 wells for standard, 1 well for blank). Subsequently, samples, standards and reagents were introduced into the wells, gently mixed at room temperature, and incubated for 1 h at 37°C. Afterwards, the liquid from each well was extracted and a detection reagent was applied. A working solution was added to each well and incubated for 1 h at 37°C once more. At the conclusion of the designated period, the solution was aspirated, and the wells were rinsed three times with 1X Wash solution. Detection reagent B working solution was applied to each well and incubated for 30 min at 37°C. Subsequent to the aspiration of the solution, the plate was washed five times with the 1X washing solution. The substrate solution was thereafter applied and incubated for 10–20 min at 37°C, protected from light. Finally the reaction was terminated using stop solution and wells were measured at 450 nm by using Biochrom EZ Read 400 Microplate reader. Curve Expert 1.4 software was used to determine the real protein concentrations.

2.7 | Biochemical Examination

Serum concentrations of Fe^{2+}, ferritin, total bilirubin, and indirect bilirubin were assessed from the rats' serum. Abbott Labs Architect C16000 systems (Abbott GmbH & Co, Germany) and commercial Abbott kits were utilized for the photometric measurement of Fe^{2+}, total bilirubin, and indirect bilirubin concentrations, while serum ferritin levels were assessed using the Chemiluminescence Analyzer UniCel DxI 800 Access Immunoassay System in conjunction with a commercial Beckman Coulter kit.

2.8 | Histopathological Analysis of the Spleen

Spleen tissue samples taken for histopathological analysis were preserved in 10% neutral formalin for 1 week. Upon completion of tissue fixation, standard histopathological processing using alcohol, xylene, and paraplast was conducted. Tissue speciments were subsequently transformed into paraffin blocks. Five-micrometer-thin sections were extracted from paraffin blocks for histopathological anlysis. Prepared sections underwent deparaffinization with xylene and were subsequently stained with hematoxylin-eosin (H&E), masson's trichome staining and toluidine blue staining. The stained sections were histological inspected using a microscope equipped with a digital camera attachment (Carl Zeiss Axiocam ERc5). Capsular fibrosis, hyperemia, structural alterations in lymph nodes, and the density of multinucleated giant and mast cells were assessed semi-quantitatively using the histologic grading method established by Hassanen et al. (2019) [24], categorized as follows: 0 (normal), 1 (mild), 2 (moderate), and 3 (severe).

In contrast, sections measuring 5 micrometers in thickness were adhered on slides treated with poly-L-lysine. After deparaffinization and rehydration with graded alcohols, antigen retrieval was performed in citrate buffer (pH 6.0) using a microwave oven at 750 W for a total of 12 min (7 min followed by 5 min). The sections were treated with Ultra V Block solution to diminish nonspecific background staining. Subsequently, they were incubated with primary antibodies targeting AKT-1 (Affinity Biosciences, Cat: AF6211, Jiangsu, China, 1:100) and PI3K (Affinity Biosciences, Cat: AF6241, Jiangsu, China, 1:100) for a duration of 60 min. Following a 30-min exposure to a secondary antibody and an additional 30 min with streptavidin–alkaline phosphatase, the slides were examined utilizing the Fast Red Substrate System. Prior to mounting with an aqueous medium, the sections were rinsed in phosphate-buffered saline and distilled water following counterstaining with Mayer's hematoxylin. A Leica DM500 light microscope was employed to examine the prepared slides and a Leica DFC295 digital camera was utilized to capture sample images. The semi-quantitative evaluation of immunoreactivity was classified according to the intensity of positive cells as very weak (+0.5), weak (+1), moderate (+2), and strong (+3) [25].

2.9 | Statistical Analysis

The data collected in the study were statistically analyzed using SPSS (SPSS Version 21.0; SPSS Inc., Chicago, IL, USA) and GraphPad Prism version 9 software (GraphPad Software Inc.; La Jolla, CA), and presented as mean ± standard deviation (SD). The Shapiro-Wilk test was employed to evaluate the normality. Given that biochemical tests, OS parameters such as MDA and GSH, and HO-1 protein levels exhibited normal distribution among the groups, a one-way ANOVA followed by the LSD test was employed for intergroup comparisons. Given the non-normal distribution of the histology score data, the non-parametric Kruskal-Wallis test, followed by Tamhane's T2 test, was utilized for intergroup comparisons. One-way ANOVA, followed by Tukey's post hoc test, was employed for group comparisons in the immunohistochemical analysis. In the statistical analysis, $p < 0.05$ was deemed significant.

3 | Results

3.1 | Oxidative Stress Biomarkers

We analyzed tissue MDA and GSH levels to assess oxidative stress in spleen tissues from the study groups and the impact of

RF and LN on OS. Figure 1 depicts the comparative analysis of spleen tissue OS biomarkers across the groups. The spleen MDA level in the RF group was significantly elevated compared to the control, DMSO, LN, and RF + LN groups ($p = 0.039$). It is evident that the RF + LN group had a reduction in the MDA levels relative to the RF group (Figure 1). Compared to the control, DMSO, LN, and RF + LN groups, GSH activity was significantly reduced in the RF group ($p = 0.028$) (Figure 1). The data indicate that RF increases OS formation, while LN has a strengthening effect on antioxidant defense mechanisms.

3.2 | Levels of HO-1 Protein

Our study also assessed the levels of HO-1, an enzyme crucial for cellular defense against oxidative damage. Figure 2 summarizes the amounts of HO-1 protein in serum and the spleen tissue. The levels of HO-1 protein were markedly elevated in the RF group relative to the control group in both serum and tissue ($p < 0.001$ and $p < 0.05$, respectively). In the RF + LN group, serum and spleen HO-1 protein levels were found to be significantly lower than those in the RF group ($p < 0.05$). These data unequivocally indicate that RF generates oxidative stress, resulting in cellular damage, and elicits an adaptive response by augmenting HO-1 activity; conversely, LN controls this oxidative damage and subsequently HO-1 production, thereby bolstering antioxidant defense.

3.3 | Results of Biochemical Analysis

The study assessed serum bilirubin, Fe^{2+}, and ferritin levels to indicate metabolic and iron homeostasis; bilirubin and Fe^{2+} were quantified via a photometric technique, whilst ferritin was determined using a chemiluminescent immunoassay. The RF group exhibited significantly elevated total bilirubin and indirect bilirubin levels in comparison to the control, DMSO, LN, and RF + LN groups ($p < 0.05$). A statistically significant

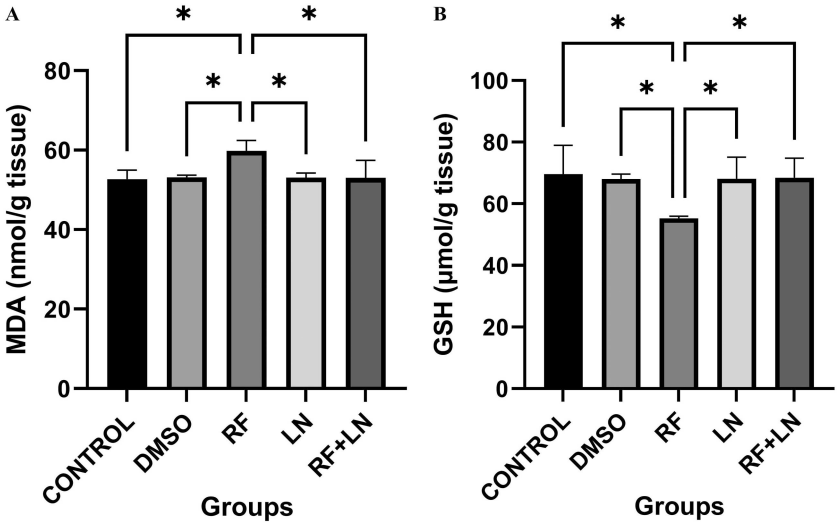

FIGURE 1 | Effects of RF and LN on oxidative stress parameters in spleen tissue. Each group represents the mean ± SD for six rats. *$p < 0.05$. DMSO, dimethyl sulfoxide; GSH, glutathione; LN, linalool; MDA, malondialdehyde; RF, rifampicin.

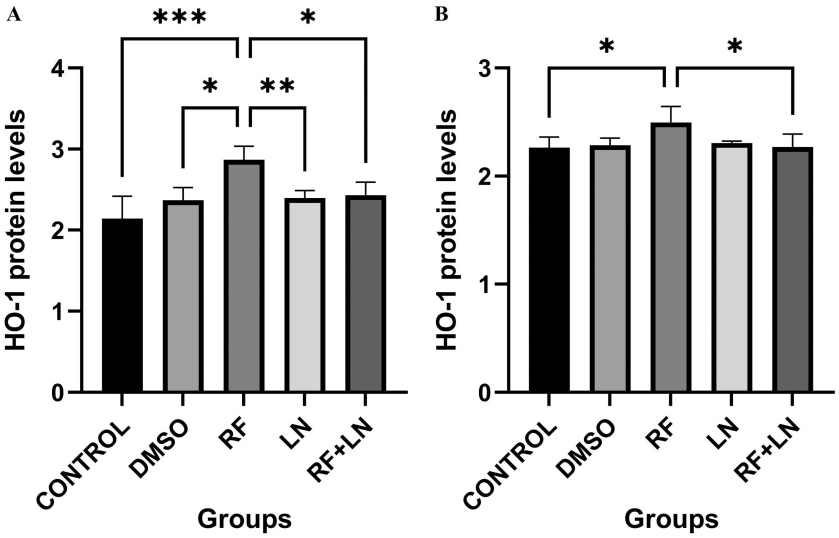

FIGURE 2 | Effect of RF and LN on HO-1 protein levels in serum (A) and spleen (B). Each group represents the mean ± SD for six rats. ***$p < 0.001$ **$p < 0.01$, *$p < 0.05$. DMSO, dimethyl sulfoxide; HO-1, heme-oxygenase 1; LN, linalool; RF, rifampicin.

decrease in total bilirubin and indirect bilirubin levels was observed when comparing the RF + LN group to the RF group ($p < 0.05$) (Figure 3A,3B). Fe^{2+} levels were significantly elevated in the RF group relative to the control and DMSO groups ($p < 0.05$). In the RF + LN group, the Fe^{2+} level was lower than in the RF group; however, this difference was not statistically significant ($p > 0.5$) (Figure 3C). The serum ferritin level in the RF group was elevated relative to the other groups; however, this increase did not reach statistical significance ($p > 0.05$) (Figure 3D).

The elevated ferritin levels in the RF group relative to other groups suggest a drug-associated inclination towards enhanced storage, albeit not statistically significant. In contrast, the more marked and significant alterations in bilirubin and Fe^{2+} in the LN group underscore LN's regulatory influence on iron metabolism.

3.4 | Histopathological Examination of the Spleen

The white pulp, red pulp, and capsule regions of splenic tissues were examined. The tissue structure in the control (Figure 4A–C; Figure 5A,F), DMSO (Figure 4D–F, Figure 5B,G), and LN (Figure 4J–L, Figure 5D,I) groups was noted to be normal. The RF group displayed larger and loosely structured white pulp, marked by a diminished quantity of nodules (Figure 4G) and the occurrence of irregularly shaped nodules (Figure 4H). Hyperemia and dilated sinusoids were observed in the red pulp (Figure 4G). The quantity of multinucleated giant cells was markedly elevated (Figure 4I), and fibrosis was seen in the capsule (Figure 5C). The density of mast cells was increased (Figure 5H). The results demonstrated statistically significant differences relative to control, DMSO, and LN groups ($p < 0.05$). In the RF + LN group, LN significantly alleviated the effects of RF ($p < 0.05$) (Figure 4M–O, Figure 5E,J) (Table 2).

Immunohistochemical analysis of spleen tissue demonstrated substantial variations in AKT-1 and PI3K expression levels between the experimental groups ($p < 0.05$). In the control and DMSO groups, immunoreactivity for AKT-1 and PI3K was minimal, with only a limited number of positively stained cells detected. Conversely, the RF group demonstrated a considerable elevation in cytoplasmic immunopositivity for both markers, which was statistically significant ($p < 0.001$). The LN group exhibited mild immunoreactivity, comparable to control levels. In the RF + LN group, the expression levels of AKT-1 and PI3K were considerably diminished compared to the RF group

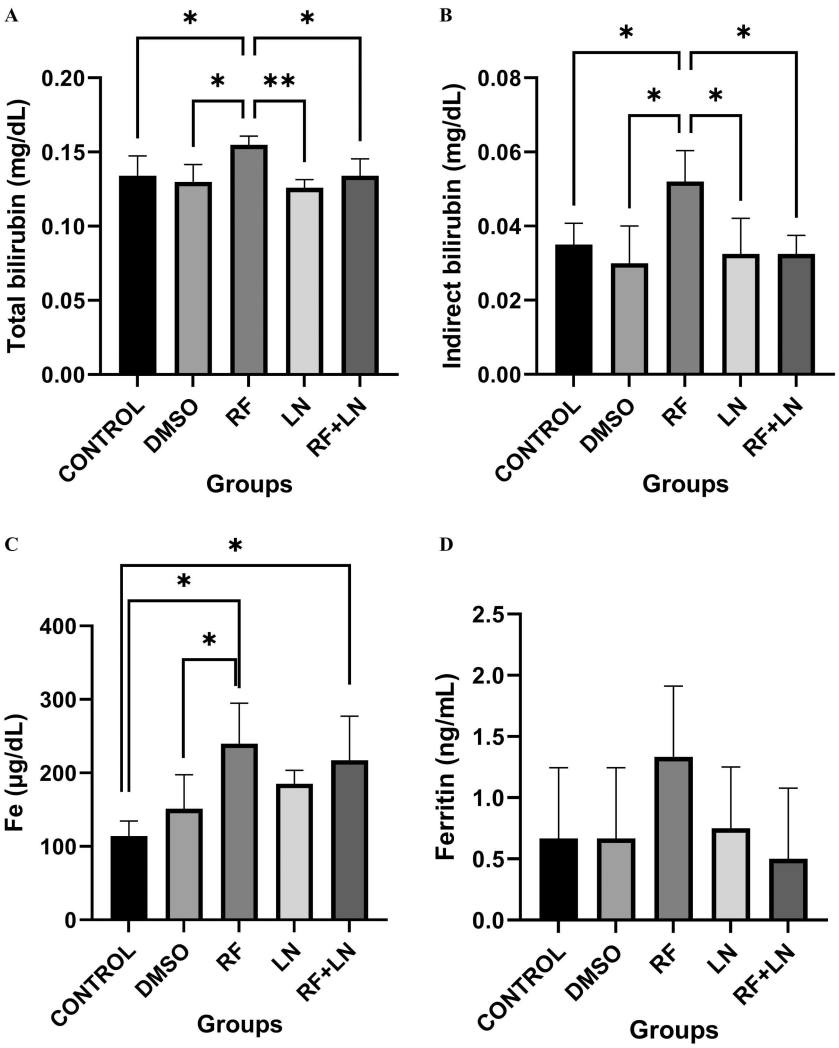

FIGURE 3 | Effects of RF and LN on total bilirubin (A), indirect bilirubin (B), Fe^{2+} (C) and ferritin (D) levels. Each group represents the mean ± SD for six rats. *$p < 0.05$, **$p < 0.01$. Fe^{2+}, iron; DMSO, dimethyl sulfoxide; LN, linalool; RF, rifampicin.

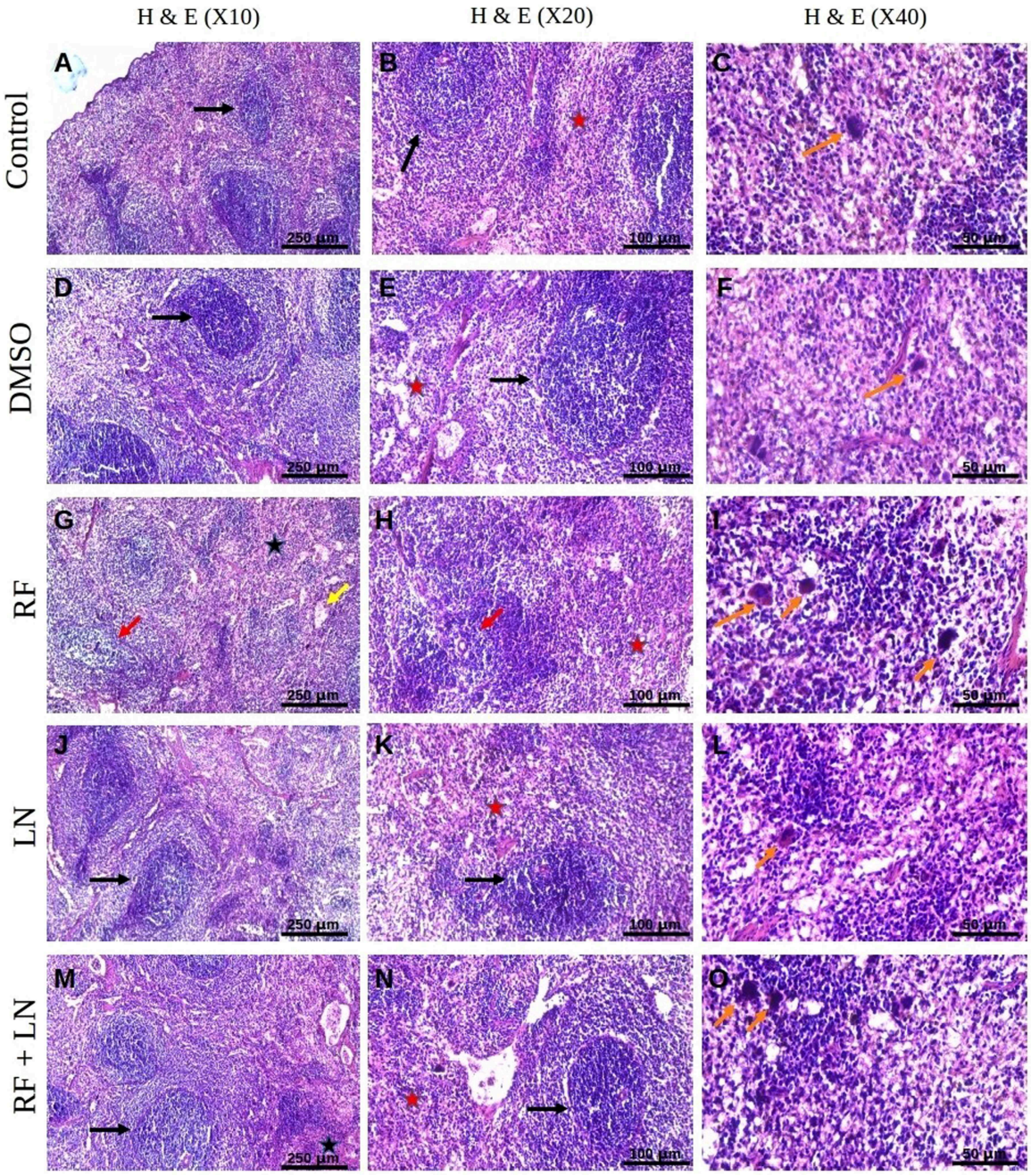

FIGURE 4 | Histological observations in splenic tissues of control and experimental groups: Normal histology of splenic tissue in control (A, B, C), DMSO (D, E, F), and LN (J, K, L); lymph node exhibiting compromised normal structure (red arrows), cords of cells comprising many lymphocytes, macrophages, and neutrophils within the red pulp (red star), alongside dilated sinusoids (yellow arrow) and hyperemia (black star) situated between these cords, and increased multinucleated giant cells density (orange arrow) in RF (G, H, I); mild histological findings in RF + LN (M, N, O). H&E × 10, × 20, and × 40. Scale bar = 250 µm, 100 µm, and 50 µm. DMSO, dimethyl sulfoxide; LN, linalool; RF, rifampicin.

($p < 0.01$), suggesting that LN treatment partially inhibited the RF-induced upregulation (Figure 6).

4 | Discussion

Approximately one-quarter of the global population is infected with *Mycobacterium tuberculosis*, and 5%–10% of these individuals will develop TB at some point in their lives [26]. Annually, almost 10 million individuals contract TB, leading to 1.3 million fatalities, constituting a significant global issue [27]. RF, recognized for its high efficacy in TB treatment, demonstrates antibacterial activity against various gram-positive cocci, including *Mycobacteria* and *Clostridium difficile*, as well as specific gram-negative organisms such as *Hemophilus influenzae*, *Neisseria meningitidis*, and *N. gonorrhoeae* [28]. The mechanisms responsible for the harmful consequences of RF treatment remain inadequately defined; nonetheless, it is widely believed that heightened inflammation, apoptosis, and OS contribute to the drug's toxicity [29]. Drug-induced tissue damage specifically leads to the impaired activity of enzymes responsible for metabolizing the drug or its components, as well as the generation of

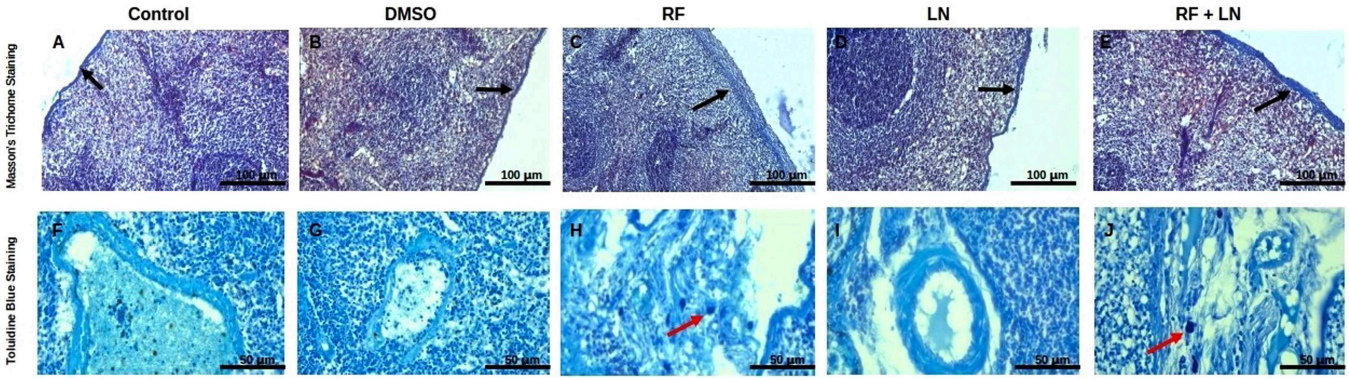

FIGURE 5 | Histological assessment of the spleen with Masson's trichrome and toluidine blue staining techniques. Normal connective tissue capsule (black arrow) and absence of mast cells in control (A, F), DMSO (B, G), and LN (D, I); capsular fibrosis and increased mast cell (red arrow) density in RF (C, H) and RF + LN (E, J). Masson's Trichome Staining, A–E; Toluidine Blue Stating, F–J. X20, Scale bar = 100 μm and 50 μm. DMSO, dimethyl sulfoxide; LN, linalool; RF, rifampicin.

TABLE 2 | Histological evaluation of spleen tissue.

Groups	Capsular fibrosis	Hiperemi	Structural defect in nodules	Giant Cell (macrophage) density	Mast cell density
Control	0.50 ± 0.548^{c}	0.83 ± 0.408^{c}	0.50 ± 0.548^{c}	$0.50 \pm 0.548^{c,e}$	$0.50 \pm 0.548^{c,e}$
DMSO	0.67 ± 0.816^{c}	0.50 ± 0.548^{c}	0.67 ± 0.516^{c}	$0.83 \pm 0.408^{c,e}$	$0.50 \pm 0.548^{c,e}$
RF	$2.67 \pm 0.516^{a,b,d}$	$2.5 \pm 0.837^{a,b,d}$	$2.5 \pm 0.837^{a,b,d}$	$2.67 \pm 0.816^{a,b,d}$	$2.67 \pm 0.516^{a,b,d}$
LN	0.67 ± 0.516^{c}	0.67 ± 0.516^{c}	0.17 ± 0.408^{c}	$0.67 \pm 0.516^{c,e}$	0.83 ± 0.753^{c}
RF + LN	1.83 ± 0.753	1.5 ± 0.837	1.5 ± 0.548	$2.33 \pm 0.816^{a,b,d}$	$1.67 \pm 0.516^{a,b}$

Note: Each group represents the mean ± SD for six rats.
Abbreviations: DMSO, dimethyl sulfoxide; LN, linalool; RF, rifampicin.
[a]Significant from control.
[b]Significant from DMSO.
[c]Significant from RF.
[d]Significant from LN.
[e]Significant from RF + LN. $p < 0.05$.

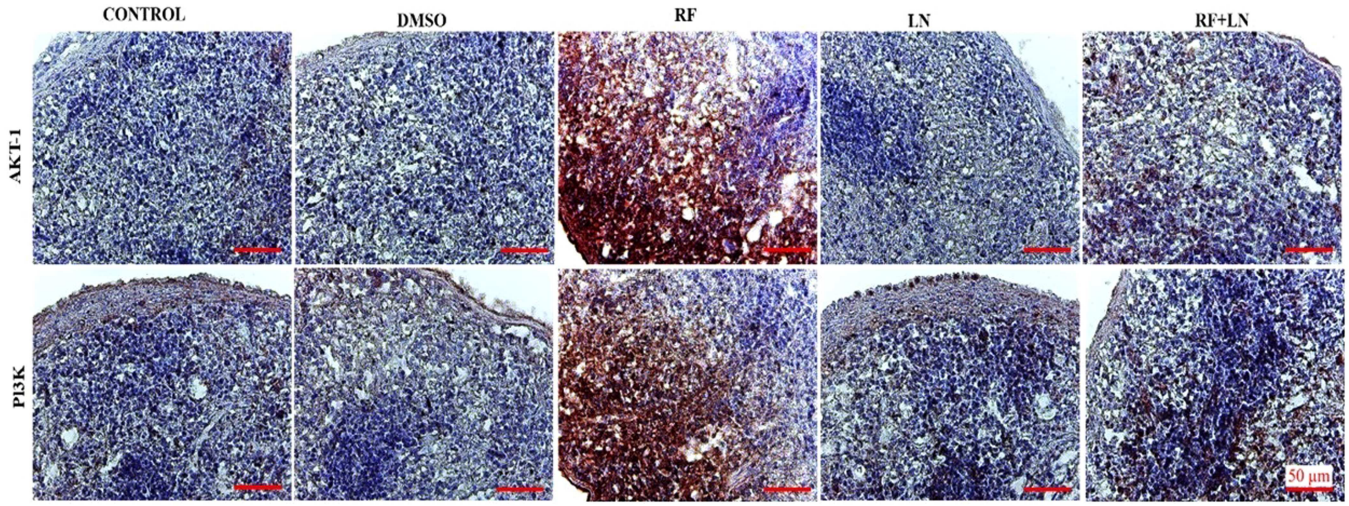

FIGURE 6 | Levels of AKT-1 and PI3K markers in the spleen of control and treated groups. (×400, Scale bar = 50 μm). AKT-1, AKT serine/threonine kinase 1; DMSO, dimethyl sulfoxide; LN, linalool; PI3K, phosphatidylinositol 3-kinase; RF, rifampicin.

reactive oxygen species (ROS), which causes damage to DNA and proteins, disrupts cellular processes, and ultimately results in cell death [30]. A study demonstrated that OS can be mitigated by both natural and synthetic antioxidants [31]. In this study, we demonstrated the protective effects of LN, a natural antioxidant prevalent in essential oils and comprising a significant portion of their composition, against RF-induced spleen damage. LN, a principal constituent of essential oils, is a monoterpene exhibiting diverse pharmacological activities, such as antibacterial, anti-inflammatory, and antioxidant actions [32].

The spleen, the largest secondary lymphoid organ in the body, is a crucial hematopoietic and immunological organ [33]. The recent recognition of the spleen's critical role in immune function has transformed the treatment of splenic disorders, promoting spleen-sparing surgery and mitigating the substantial risk of sepsis following total splenectomy [34]. Studies indicate that the administration of anti-TB drugs including RF, INH, and pyrazinamide, results in elevated levels of ROS in the spleen, diminished GSH and protein content, and hemophagocytic lymphohistiocytosis, alongside notable alterations in hematological parameters, DNA fragmentation, and chromosomal integrity [6, 35]. Anti-TB drugs have been demonstrated to elicit peripheral neuritis, gastrointestinal disturbances, and acute drug-induced hepatic injury, accompanied by the elevation of reactive nitrogen species, resulting in splenic tissue damage [36, 37].

HO-1 primarily degrades heme and functions as the rate-limiting enzyme in the synthesis of CO, Fe^{2+}, and biliverdin, which is subsequently converted to bilirubin [38]. Our results align with studies indicating that elevated HO-1 levels due to RF treatment enhance excessive production of ROS, heme derivative CO, total bilirubin, indirect bilirubin, Fe^{2+}, and Fe^{2+}-dependent lipid peroxidation, thereby disrupting iron metabolism and exacerbating tissue damage, leading to ferroptosis and hyperbilirubinemia [39–43]. Ferroptosis is identified as a novel form of iron-dependent programmed cell death, separate from apoptosis, necroptosis, and autophagy, characterized by the accumulation of Fe^{2+}, ROS, and lipid peroxides, alongside GSH depletion and glutathione peroxidase 4 (GPX4) inactivation [44]. Fe^{2+} accumulation is a crucial mediator of various cytotoxic pathways that result in the breakdown of redox homeostasis and subsequent cell death [45]. The primary function of ferritin is to bind Fe^{2+}, oxidize it, and release Fe^{2+} in accordance with cellular requirements. Consistent with prior research, our study demonstrated that tissue damage arises from elevated Fe^{2+} levels in cells, prompting an increase in ferritin levels to facilitate the transport of released Fe^{2+} back into the serum [46, 47]. Research indicates that elevated ferritin levels correlate with various conditions, including inflammation, infection, metabolic disorders, hemophagocytic lymphohistiocytosis, and malignancies [48]. A study's results indicate that cells are predisposed to ferroptosis when the rise in ferritin is lower than the increase in Fe^{2+}, aligning with our findings [49].

LN, prossessing antioxidant properties and utilized in this research, mitigated OS and inhibited HO-1, markedly enhancing Fe^{2+} production and Fe^{2+}-dependent lipid peroxidation, as well as total and indirect bilirubin levels. We noted an enhancement in HO-1 levels in the RF + LN group versus to the RF group. Our results align with the study's findings, which indicated that elevated ROS levels were mitigated by the antioxidant defense system [50]. The results of numerous research indicating that natural substances are used alongside medications to maintain balanced HO-1 levels align with our results. For instance, a study concluded that anti-inflammatory procyanidin supplementation effectively mitigates inflammation by modulating HO-1, inhibiting the production of inflammatory cytokines, and reducing ferroptosis [51]. A separate study shown that puerarin, an antioxidant, inhibits ROS generation and ferroptosis by decreasing HO-1 levels while elevating GSH and GPX4 levels within the cell [52]. Our findings align with studies indicating that the inhibition of HO-1 elevates GPX4 levels, markedly enhances cell viability by mitigating OS, lipid peroxidation, and ferroptosis, while also decreasing intracellular Fe^{2+} accumulation [53, 54]. A further investigation, aligning with our results, indicated that quercetagetin, with antioxidant characteristics, markedly diminished the elevations in total bilirubin levels by decreasing zearalenone-induced OS [55].

The present study revealed that RF elevated MDA levels, a lipid peroxide, in spleen tissue by compromising cell membranes via excessive ROS production, while concurrently diminishing GSH enzyme activity, the primary antioxidant in the body that protects against free radicals, in comparison to the control group. Our results align with prior research indicating that RF treatment markedly elevates lipid peroxidation while diminishing antioxidant activities, including GSH, superoxide dismutase, and catalase [56, 57]. Our present investigation aligns with findings indicating that HO-1 overexpression leads to elevated ROS and Fe^{2+} generation, as well as heightened MDA levels, ultimately inducing ferroptosis due to GPX4 depletion [58]. Our work demonstrated that LN diminishes MDA generation and enhances the activity of the antioxidant enzyme GSH. Research indicates that LN, a monoterpene, neutralizes free radicals owing to its antioxidant, antibacterial, antiviral, and enzyme inhibitory activities [59]. LN prossesses antioxidant and anti-inflammatory characteristics, which may elucidate its beneficial effects on the spleen.

The present work revealed that alterations in indicators of RF-induced oxidative damage, assessed using biochemical and ROS measures, aligned with our histological and immunohistochemical observations in spleen tissue. A study shown that HO1 activity is modulated by the PI3K/Akt signaling pathway [60]. Numerous studies have shown that the PI3K/AKT/HO-1 pathway is linked to ferroptosis, and the inhibition of ferroptosis may serve as a therapeutic target for mitigating OS and inflammation [61, 62]. Consequently, in our investigation, we assessed the correlation between splenic damage and the PI3K/AKT/HO-1 signaling pathway. A separate study indicated that aberrant activation of various signaling pathways, such as PI3K/AKT/mTOR and Nrf2/HO-1, initiates pathological processes, and that modulation of these pathways can effectively suppress inflammatory responses and enhance OS by addressing immune imbalance [63]. The findings of our study, which indicated elevated Fe^{2+} release resulting from heightened erythrophagocytosis in compromised red pulp macrophages within the spleen, alongside enhanced ROS and lipid peroxidation linked to ferroptosis, align with the outcomes of a prior investigation [64]. Our findings align with numerous studies that identified pathological features, including loosely organized lymphocyte clusters in the white pulp, hyperemia, and dilated sinusoids populated by lymphocytes, macrophages, and neutrophils in the red pulp, as well as multinucleated giant cells, fibrosis, and hightened mast cell density in the RF-treated groups [65, 66]. Moreover, our results demonstrated statistically significant elevations in PI3K and Akt1 immunoreactivity in the RF group relative to the control group. Numerous studies indicate that the stimulation of the PI3K/AKT pathway results in mitochondrial malfunction, OS, and accelerated aging [67, 68]. Our results align with a study indicating that RF

induces organ damage through OS [69]. A separate study indicated that the simultaneous administration of three critical antituberculosis medications, rifampicin, isoniazid, and pyrazinamide, resulted in damage to the spleen, blood, and bone marrow, specifically affecting hematological parameters, alongside genetic damage including DNA fragmentation and chromosomal abnormalities [6].

We detected substantial decreases in these histological and immunohistochemical alterations following LN therapy. Our findings indicate that LN safeguards against RF-induced histological and immunohistochemical alterations in splenic tissue. Our results align with studies indicating that antioxidants help mitigate tissue damage resulting from OS. A study shown that barley, an antioxidant, safeguards spleen tissues against alterations like macrophage infiltration, fibrinoid deposition, hyperemia, dilated sinusoids, and structural damage in both white and red pulp, corroborating our findings [70]. Our results align with prior research indicating that ferrostatin-1, a ferroptosis inhibitor, mitigated the elevations in ROS and lipid peroxidation by obstructing the release of Fe^{2+} and ferroptosis in compromised red pulp macrophages [64]. Our data indicate that LN enhanced ROS homeostasis in cells affected by RF, fortified antioxidant defenses, and inhibited HO-1-mediated ferroptosis, thereby preventing tissue damage in the spleen.

Our results align with a study indicating that the antioxidant curcumin mitigates inflammation and OS by decreasing PI3K/AKT and NF-κB activation [71]. A further investigation demonstrated that the antioxidant 3,5,6,7,8,3',4'-hepmethoxyflavone markedly suppressed PI3K/AKT levels and diminished OS [72]. The research demonstrated that phillygenin, an anti-inflammatory and antioxidant compound, inhibited bleomycin-induced lung fibrosis by suppressing the PI3K-Akt-mTOR signaling pathway [73]. Our findings indicate that LN mitigates RF-induced immunotoxicity by diminishing OS and modulating the PI3K/AKT signaling pathway.

The results of this study indicate that targeting HO-1 and the PI3K/AKT pathway may represent a feasible approach for treating some illnesses. It is essential to acknowledge the physiological thresholds for HO-1 and PI3K/AKT levels. Additionally, targeting HO-1 and PI3K/AKT-mediated ROS may uncover novel ways to alleviate RF-induced cellular damage. In conclusion, the mechanism of RF-induced splenic injury likely involves OS pathways; this damage to splenic tissue may be mitigated with the therapeutic administration of antioxidant medicines such as LN. Nonetheless, additional clinical trials are need to validate this compelling hypothesis.

Author Contributions

Ayşegül Acet: methodology, writing – review and editing, investigation. **Sebile Azırak:** writing – original draft, methodology, visualization, writing – review and editing, formal analysis, conceptualization, investigation, validation. **Ebru Annaç:** methodology, writing – original draft, visualization, writing – review and editing; investigation. **Halime Tozak Yıldız:** investigation, writing – original draft, methodology, visualization, writing – review and editing. **İbrahim Bozgeyik:** methodology, investigation. **Deniz Taştemir Korkmaz:** writing – original draft; funding acquisition, visualization, methodology, writing – review and editing, validation, project administration, conceptualization, investigation, supervision.

Acknowledgments

This research was undertaken as a master's thesis at the Department of Medical Biology, Faculty of Medicine, Adıyaman University, Adıyaman/TURKEY. We would like to express our gratitude to technician Nurhan TIRAŞÇI from the Adıyaman University Experimental Animal Production, Application and Research Center for her assistance.

Data Availibility Statement

Data available on request from the authors.

References

1. World Health Organization. Global Tuberculosis Report 2023, accessed April 28, 2025, https://www.who.int/publications/i/item/9789240083851.

2. I. S. Padda and K. M. Reddy, "Antitubercular Medications." *StatPearls* (Treasure Island (FL): StatPearls Publishing, 2024).

3. R. Sharma, R. Kaur, M. Mukesh, and V. L. Sharma, "Assessment of Hepatotoxicity of First-Line Anti-Tuberculosis Drugs on Wistar Rats," *Naunyn-Schmiedeberg's Archives of Pharmacology* 391, no. 1 (2018): 83–93.

4. S. Goutelle, L. Bourguignon, P. H. Maire, M. Van Guilder, J. E. Conte, and R. W. Jelliffe, "Population Modeling and Monte Carlo Simulation Study of the Pharmacokinetics and Antituberculosis Pharmacodynamics of Rifampin in Lungs," *Antimicrobial Agents and Chemotherapy* 53, no. 7 (2009): 2974–2981.

5. X. Zhuang, L. Li, T. Liu, et al., "Mechanisms of Isoniazid and Rifampicin-Induced Liver Injury and the Effects of Natural Medicinal Ingredients: A Review," *Frontiers in Pharmacology* 13 (2022): 1037814.

6. R. Sharma and V. L. Sharma, "Deleterious Effects of 28-Day Oral Co-Administration of First-Line Anti-TB Drugs on Spleen, Blood and Bone Marrow Chromosomes in Normal Rat," *Drug and Chemical Toxicology* 40 (2017): 154–163.

7. L. Li, M. Duan, W. Chen, et al., "The Spleen in Liver Cirrhosis: Revisiting an Old Enemy With Novel Targets," *Journal of Translational Medicine* 15, no. 1 (2017): 111.

8. S. T. Fraser, R. G. Midwinter, B. S. Berger, and R. Stocker, "Heme Oxygenase-1: A Critical Link Between Iron Metabolism, Erythropoiesis, and Development," *Advances in Hematology* 2011 (2011): 1–6.

9. Q. Xiao, R. Piao, H. Wang, C. Li, and L. Song, "Orientin-Mediated Nrf2/HO-1 Signal Alleviates H2O2-Induced Oxidative Damage via Induction of JNK and PI3K/AKT Activation," *International Journal of Biological Macromolecules* 118, no. Pt A (2018): 747–755.

10. B. Ren, M. Wang, D. Hao, Z. Wang, and L. Dai, "Dendrobium Officinale Extract Alleviates Aging-Induced Kidney Injury by Inhibiting Oxidative Stress via the PI3K/Akt/Nrf2/HO-1 Pathway," *Journal of Ethnopharmacology* 352 (2025): 120156.

11. L. L. Ma, L. Sun, Y. X. Wang, B. H. Sun, Y. F. Li, and Y. L. Jin, "Association Between HO-1 Gene Promoter Polymorphisms and Diseases (Review)," *Molecular Medicine Reports* 25, no. 1 (2021): 29.

12. S. H. Hosseini, H. Bibak, A. R. Ghara, A. Sahebkar, and A. Shakeri, "Ethnobotany of the Medicinal Plants Used by the Ethnic Communities of Kerman Province, Southeast Iran," *Journal of Ethnobiology and Ethnomedicine* 17, no. 1 (2021): 31.

13. S. Azırak, "Prevention of Nephrotoxicity Induced by Amikacin: The Role of Misoprostol, A Prostaglandin E1 Analogue," *Prostaglandins & Other Lipid Mediators* 164 (2023): 106682, https://doi.org/10.1016/j.prostaglandins.2022.106682.

14. S. Azırak, S. Bilgiç, D. T. Korkmaz, I. Armağan, and M. Ö. Kaya, "Thymoquinone Prevents Valproic Acid-Induced Hepatotoxicity via Modulation of Cytochrome P450, PPARs, and Apoptotic Pathways," *Iranian Journal of Basic Medical Sciences* 28, no. 7 (2025): 899–906.

15. D. Taştemir Korkmaz, S. Bilgiç, S. Azırak, A. N. Güvenç, N. Kocaman, and M. K. Özer, "The Protective Effect of Resveratrol Against Risperidone-Induced Brain Damage and Metabolic Side Effects," *Cukurova Medical Journal* 43 (2018): 108–123.

16. O. S. Ola and T. A. Sofolahan, "A Monoterpene Antioxidant, Linalool, Mitigates Benzene-Induced Oxidative Toxicities on Hematology and Liver of Male Rats," *Egyptian Journal of Basic and Applied Sciences* 8, no. 1 (2021): 39–53.

17. F. Guo, Q. Chen, Q. Liang, et al., "Antimicrobial Activity and Proposed Action Mechanism of Linalool Against Pseudomonas Fluorescens," *Frontiers in Microbiology* 12 (2021): 562094.

18. W. Mączka, A. Duda-Madej, M. Grabarczyk, and K. Wińska, "Natural Compounds in the Battle Against Microorganisms-Linalool," *Molecules* 27, no. 20 (2022): 6928.

19. M. Özgöçmen and S. Azirak, "The Curative Role of Linalool In Rifampicin-Induced Brain Tissue Damage," *SDÜ Med J SDU* 30, no. 3 (2023): 362–370.

20. T. Hussain, G. Subaiea, and H. Firdous, "Hepatoprotective Evaluation of Trapa Natans Against Drug-Induced Hepatotoxicity of Antitubercular Agents in Rats," *Pharmacognosy Magazine* 14, no. 54 (2018): 180–185.

21. E. Altinoz, Z. Oner, H. Elbe, N. Uremis, and M. Uremis, "Linalool Exhibits Therapeutic and Protective Effects in a Rat Model of Doxorubicin-Induced Kidney Injury by Modulating Oxidative Stress," *Drug and Chemical Toxicology* 45, no. 5 (2022): 2024–2030.

22. Z. A. Placer, L. L. Cushman, and B. C. Johnson, "Estimation of Product of Lipid Peroxidation (Malonyldialdehyde) in Biochemical Systems," *Analytical Biochemistry* 16, no. 2 (1966): 359–364.

23. G. L. Ellman, "Tissue Sulfhydryl Groups," *Archives of Biochemistry and Biophysics* 82 (1959): 70–77.

24. E. I. Hassanen, A. A. Khalaf, A. F. Tohamy, E. R. Mohammed, and K. Y. Farroh, "Toxicopathological and Immunological Studies on Different Concentrations of Chitosan- Coated Silver Nanoparticles in Rats," *International Journal of Nanomedicine* 14 (2019): 4723–4739.

25. A. Turk, T. O. Metin, T. Kuloglu, et al., "Isthmin-1 and Spexin as Promising Novel Biomarker Candidates for Invasive Ductal Breast Carcinoma," *Tissue & Cell* 91 (2024): 102601.

26. A. Vasiliu, L. Martinez, R. K. Gupta, et al., "Tuberculosis Prevention: Current Strategies and Future Directions," *Clinical Microbiology and Infection* 30, no. 9 (2024): 1123–1130.

27. V. Singh, "Tuberculosis Treatment-Shortening," *Drug Discovery Today* 29, no. 5 (2024): 103955.

28. Suresh A. Beloor, A. Rosani, P. Patel, and W. R. Rifampin In: StatPearls. Treasure Island (FL): StatPearls Publishing LLC; 2024.

29. J. Rani, S. B. Dhull, P. K. Rose, and M. K. Kidwai, "Drug-Induced Liver Injury and Anti-Hepatotoxic Effect of Herbal Compounds: A Metabolic Mechanism Perspective," *Phytomedicine* 122 (2024): 155142.

30. A. Mili, S. Birangal, K. Nandakumar, and R. Lobo, "A Computational Study to Identify Sesamol Derivatives as NRF2 Activator for Protection Against Drug-Induced Liver Injury (DILI)," *Molecular Diversity* 28, no. 3 (2024): 1709–1731.

31. A. Ishtiaq, I. Mushtaq, H. Rehman, et al., "Tetra Aniline-Based Polymers Ameliorate BPA-Induced Cardiotoxicity in Sprague Dawley Rats, in Silico and In Vivo Analysis," *Life Sciences* 358 (2024): 123104.

32. S. Kaya and T. Yalçın, "Linalool May Have a Therapeutic Effect on Cadmium-Induced Nephrotoxicity by Regulating NF-κB/TNF and GRP78/CHOP Signaling Pathways," *Journal of Trace Elements in Medicine and Biology* 86 (2024): 127510.

33. Z. Huang, K. Sun, Z. Luo, et al., "Spleen-Targeted Delivery Systems and Strategies for Spleen-Related Diseases," *Journal of Controlled Release* 370, no. 370 (2024): 773–797.

34. H. Lazaar, Y. Malki, T. Bouhout, B. Serji, and T. El Harroudi, "Partial Splenectomy for a Sizeable Cavernous Hemangioma: Case Report and a Review of the Literature," *Cureus* 13, no. 1 (2021): e12882.

35. C. Wang, J. Qiu, X. Huang, J. Xu, and L. Pan, "Hemophagocytic Lymphohistiocytosis Secondary to Rifampin Treatment: A Case Report," *Medicine* 103, no. 29 (2024): e39011.

36. X. Liu, Y. Ma, Y. Liu, et al., "Near-Infrared Molecular Sensor for Visualizing and Tracking ONOO(-) During the Process of Anti-Tuberculosis Drug-Induced Liver Damage," *Analytical and Bioanalytical Chemistry* 415, no. 29–30 (2023): 7187–7196.

37. Y. Zheng, B. Cui, W. Sun, et al., "Potential Crosstalk Between Liver and Extra-Liver Organs in Mouse Models of Acute Liver Injury," *International Journal of Biological Sciences* 16, no. 7 (2020): 1166–1179.

38. Y. T. Liu, Z. M. Lin, S. J. He, and J. P. Zuo, "Heme Oxygenase-1 as a Potential Therapeutic Target in Rheumatic Diseases," *Life Sciences* 218 (2019): 205–212.

39. L. C. Chang, S. K. Chiang, S. E. Chen, Y. L. Yu, R. H. Chou, and W. C. Chang, "Heme oxygenase-1 Mediates BAY 11-7085 Induced Ferroptosis," *Cancer Letters* 416 (2018): 124–137.

40. D. Y. Hou, J. J. Lu, X. Zhang, et al., "Heme Metabolism and HO-1 in the Pathogenesis and Potential Intervention of Endometriosis," *American Journal of Reproductive Immunology* 91, no. 5 (2024): e13855.

41. B. Perumal Kannabiran, N. A. Palaniappan, T. Manoharan, et al., "Safety and Efficacy of 25 mg/kg and 35 mg/kg vs. 10 mg/kg Rifampicin in Pulmonary TB: A Phase IIb Randomized Controlled Trial," *Open Forum Infectious Diseases* 11, no. 3 (2024): ofae034.

42. H. M. Schipper, W. Song, A. Tavitian, and M. Cressatti, "The Sinister Face of Heme Oxygenase-1 in Brain Aging and Disease," *Progress in Neurobiology* 172 (2019): 40–70.

43. S. Yang, J. Ouyang, Y. Lu, V. Harypursat, and Y. Chen, "A Dual Role of Heme Oxygenase-1 in Tuberculosis," *Frontiers in Immunology* 13 (2022): 842858.

44. M. Xu, D. Zhang, and J. Yan, "Targeting Ferroptosis Using Chinese Herbal Compounds to Treat Respiratory Diseases," *Phytomedicine* 130 (2024): 155738.

45. D. Mancardi, M. Mezzanotte, E. Arrigo, A. Barinotti, and A. Roetto, "Iron Overload, Oxidative Stress, and Ferroptosis in the Failing Heart and Liver," *Antioxidants (Basel, Switzerland)* 2021 10, no. 12 (2021): 1864.

46. Z. Jin, H. Zhang, L. Bai, et al., "Synovium Is a Sensitive Tissue for Mapping the Negative Effects of Systemic Iron Overload in Osteoarthritis: Identification and Validation of Two Potential Targets," *Journal of Translational Medicine* 21, no. 1 (2023): 661.

47. I. A. Malik, J. Wilting, G. Ramadori, and N. Naz, "Reabsorption of Iron into Acutely Damaged Rat Liver: A Role for Ferritins," *World Journal of Gastroenterology* 23, no. 41 (2017): 7347–7358.

48. S. K. Ing, G. W. C. Lee, T. S. Leong, et al., "Secondary Hemophagocytic Lymphohistiocytosis: An Unusual Complication in Disseminated Mycobacterium Tuberculosis," *Clinical Medicine* 23, no. 4 (2023): 414–416.

49. X. Lin, X. Zhao, Q. Chen, X. Wang, Y. Wu, and H. Zhao, "Quercetin Ameliorates Ferroptosis of Rat Cardiomyocytes via Activation of the SIRT1/p53/SLC7A11 Signaling Pathway to Alleviate Sepsis-Induced Cardiomyopathy," *International Journal of Molecular Medicine* 52, no. 6 (2023): 116.

50. A. Tyagi, S. Haq, and S. Ramakrishna, "Redox Regulation of DUBs and Its Therapeutic Implications in Cancer," *Redox Biology* 48 (2021): 102194.

51. J. Zeng, Y. Weng, T. Lai, et al., "Procyanidin Alleviates Ferroptosis and Inflammation of LPS-Induced RAW264.7 Cell via the Nrf2/HO-1 Pathway," *Naunyn-Schmiedeberg's Archives of Pharmacology* 397, no. 6 (2024): 4055–4067.

52. X. Yue, M. Pang, Y. Chen, et al., "Puerarin Alleviates Symptoms of Preeclampsia Through the Repression of Trophoblast Ferroptosis via the CREB/HO-1 Pathway," *Placenta* 158 (2024): 145–155.

53. Z. Tang, Y. Ju, X. Dai, et al., "HO-1-Mediated Ferroptosis as a Target for Protection Against Retinal Pigment Epithelium Degeneration," *Redox Biology* 43 (2021): 101971.

54. H. Zhou, B. Li, Z. Wang, et al., "HO-1-mediated Ferroptosis Regulates Retinal Neovascularization via the COX2/VEGFA Axis," *Free Radical Biology and Medicine* 226 (2025): 84–95.

55. F. Wu, F. Wang, Z. Tang, et al., "Quercetagetin Alleviates Zearalenone-Induced Liver Injury in Rabbits Through Keap1/Nrf2/ARE Signaling Pathway," *Frontiers in Pharmacology* 14 (2023): 1271384.

56. T. Anwer, M. N. Alruwaili, S. Alshahrani, et al., "Hepatoprotective Potential of Diosmin Against Hepatotoxic Effect of Isoniazid and Rifampin in Wistar Rats," *Human and Experimental Toxicology* 42 (2023): 1–10.

57. Y. Sun, Y. Zhang, N. Ma, and S. Cai, "Rhus Chinensis Mill. Fruits Alleviate Liver Injury Induced by Isoniazid and Rifampicin Through Regulating Oxidative Stress," *Journal of Ethnopharmacology* 310 (2023): 116387.

58. C. Lu, Z. Zhang, Y. Fan, X. Wang, J. Qian, and Z. Bian, "Shikonin Induces Ferroptosis in Osteosarcomas Through the Mitochondrial ROS-Regulated HIF-1α/HO-1 Axis," *Phytomedicine* 135 (2024): 156139.

59. K. A. Wojtunik-Kulesza and A. Oniszczuk, "Ability of Selected Monoterpenes to Reduce Fe(III) Ions Being Pro-Neurodegenerative Factors: Tests Based on a FRAP Reaction Extended to 48 Hours," *International Journal of Molecular Sciences* 25, no. 4 (2024): 2191.

60. J. Tian, Y. Li, X. Mao, et al., "Effects of the PI3K/Akt/HO-1 Pathway on Autophagy in a Sepsis-Induced Acute Lung Injury Mouse Model," *International Immunopharmacology* 124, no. Pt B (2023): 111063.

61. Y. He, Y. Wang, H. Duan, et al., "Pharmacological Targeting of Ferroptosis in Hypoxia-Induced Pulmonary Edema: Therapeutic Potential of Ginsenoside Rg3 Through Activation of the PI3K/AKT Pathway," *Frontiers in Pharmacology* 16 (2025): 1644436.

62. J. Huang, Q. Li, H. Wang, et al., "Betulinic Acid Inhibits Glioma Progression by Inducing Ferroptosis Through the PI3K/Akt and NRF2/HO-1 Pathways," *The Journal of Gene Medicine* 27, no. 2 (2025): e70011.

63. M. Zhang, D. Pu, F. Meng, G. Shi, and J. Li, "Alterations in Signaling Pathways and Therapeutic Strategies of Traditional Chinese Medicine in Granulomatous Lobular Mastitis," *Journal of Inflammation Research* 18 (2025): 9185–9197.

64. L. A. Youssef, A. Rebbaa, S. Pampou, et al., "Increased Erythrophagocytosis Induces Ferroptosis in Red Pulp Macrophages in a Mouse Model of Transfusion," *Blood* 131, no. 23 (2018): 2581–2593.

65. R. H. Dosh, S. M. Al-Rehemi, M. J. Frayyeh, R. H. Al Mudhafar, and H. Abdulkadhim, "Histopathological, Immunohistochemical and Physiological Study for the Hepatoprotective Effect of Melatonin Against Inhrifampicin-Induced Hepatotoxicity in Mice Model," *Wiadomości Lekarskie* 77, no. 9 (2024): 1745–1752.

66. X. He, Y. Song, L. Wang, and J. Xu, "Protective Effect of Pyrrolidine Dithiocarbamate on Isoniazid/Rifampicin-Induced Liver Injury in Rats," *Molecular Medicine Reports* 21, no. 1 (2020): 463–469.

67. R. M. Abdelsalam, H. W. Hamam, N. M. Eissa, A. E. El-Sahar, and R. M. Essam, "Empagliflozin Dampens Doxorubicin-Induced Chemobrain in Rats: The Possible Involvement of Oxidative Stress and PI3K/Akt/mTOR/NF-κB/TNF-α Signaling Pathways," *Molecular Neurobiology* 62, no. 3 (2025): 3480–3492.

68. P. Zhang, N. Zhang, Y. Hu, et al., "Role of PI3K/AKT/MAOA in Glucocorticoid-Induced Oxidative Stress and Associated Premature Senescence of the Trabecular Meshwork," *Aging cell* 24, no. 4 (2025): e14452.

69. P. Shivaji and S. E. Prince, "Unveiling the Molecular Toxicity of Isoniazid and Rifampicin in Tuberculosis Therapy: Emerging Insights and Therapeutic Strategies," *Toxicology Mechanisms and Methods* 35, no. 9 (2025): 1239–1270.

70. M. Shehata, H. Saad Eldien, F. Meligy, and S. Bahaidarh, "The Possible Protective Role of Barley Seeds on the Spleen After Administration of Glucocorticoids in Adult Albino Rats: A Histological and Immunohistochemical Study," *Journal of Microscopy and Ultrastructure* 7, no. 4 (2019): 171–180.

71. K. Liu, M. Shi, X. Li, X. Zeng, and X. Liu, "Curcumin Modulates the PTEN/PI3K/AKT Pathway to Alleviate Inflammation and Oxidative Stress in PM2.5-Induced Chronic Obstructive Pulmonary Disease," *Food and Chemical Toxicology* 201 (2025): 115460.

72. Y. Wang, Z. Ma, W. Peng, et al., "3,5,6,7,8,3',4'- Heptamethoxyflavonoid Inhibits TGF-β1-induced Epithelial-Mesenchymal Transition by Regulating Oxidative Stress and Autophagy Through MEK/ERK/PI3K/AKT/mTOR Signaling Pathway," *Scientific Reports* 15, no. 1 (2025): 4567.

73. Y. Wei, W. Ni, L. Zhao, et al., "Phillygenin Inhibits PI3K-Akt-mTOR Signalling Pathway to Prevent Bleomycin-Induced Idiopathic Pulmonary Fibrosis in Mice," *Clinical and Experimental Pharmacology and Physiology* 52, no. 2 (2025): e70017.